

Characterization of the aluminum models of the 3.9GHz separators for a K⁺ beam at Fermilab.

Leo Bellantoni
April 20, 2000

Abstract

This note describes measurements made on the Al models of 3.9GHz RF separators made for the R & D effort to develop a separated K⁺ beam at Fermilab. It details the basic measurement technique, describes various uncertainties in the measurement, and provides the results of measurements on the single elliptical dumbbell as well as a stack of 4 unpolarized dumbbells. Measurements of the spectra, Q, and bead pull results are given.

1) Measurement apparatus

The models were studied using the old linac bead pull apparatus and a Hewlett-Packard model 8510C network analyzer. Credit for reviving this apparatus belongs largely with *Flora, Prieto, et.al.* An Apple G3 running Labview, connected to the 8510 with an HP-IB interface and to the bead pull motor controller with a serial port was used to collect the data in a spreadsheet format. The motor controller was upgraded to a Galil model DMC-1412 which has been operated in a stepper-motor configuration; the Apple USP serial port interfaces to the Galil unit through a USP/RS-232 adapter from Griffin. Figures 1 and 2 provide simple sketches of the apparatus. Three “beads” are in use:

- a) An irregularly shaped plastic bead which is roughly a donut of 2.2mm diameter, 2.0mm height and of unknown dielectric constant.
- b) A brass sphere, 3.04mm diameter drilled to 1.28mm diameter and of nominally 10.9 cubic millimeter volume.
- c) A steel needle, of 3.60 length and 0.70mm diameter and nominally 1.09 cubic millimeter volume.

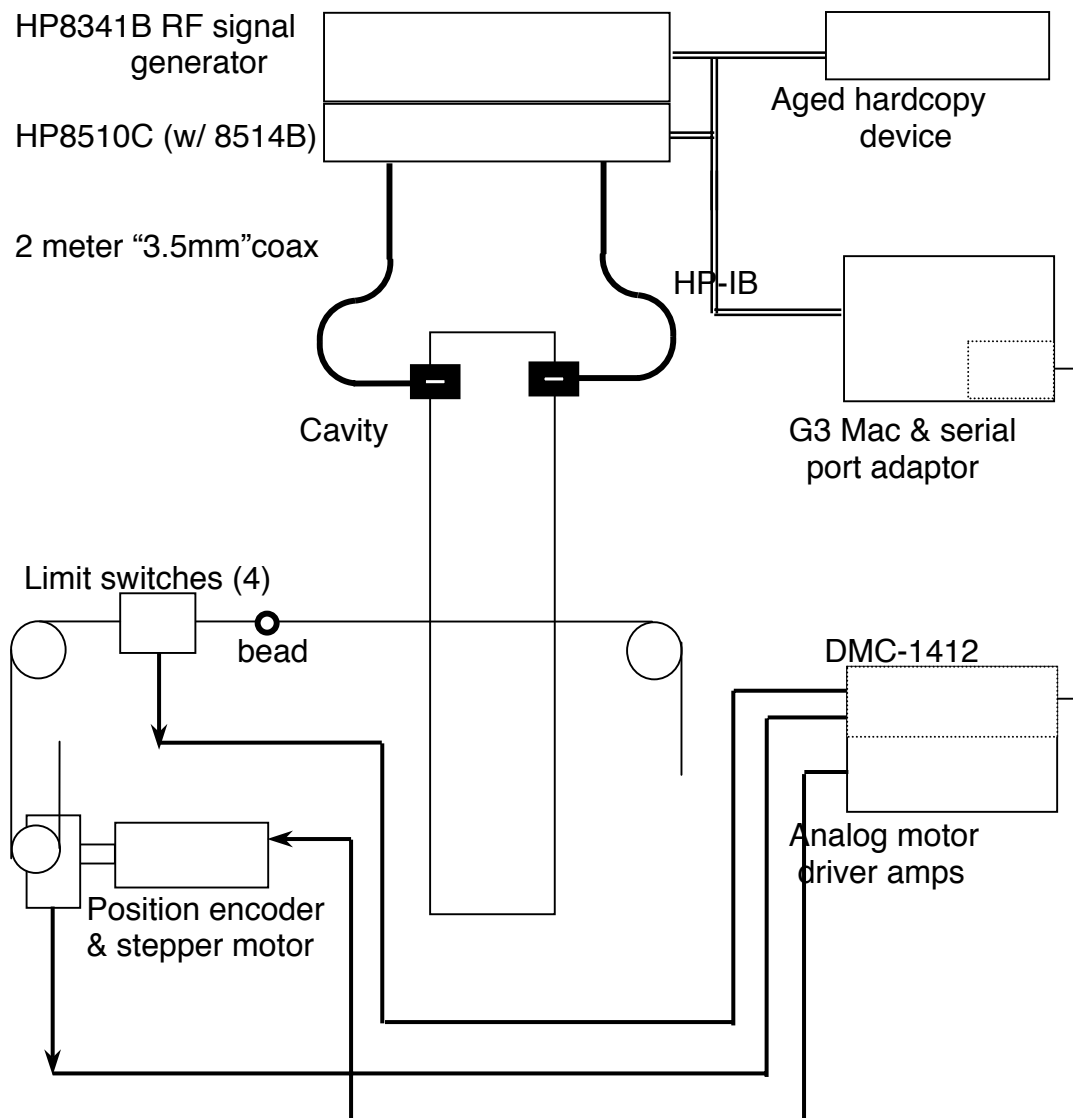


Figure 1. The bead pull apparatus.

At this time the endplates have holes large enough to pass a bead through at only two points, one of which is the centerline of the system. The thread itself is located in the hole by eye, and that positioning is good to better than a half millimeter. The longitudinal position of the thread is read out by the stepper motor with a tremendous precision. However, vibrations of the string and bead shape irregularities limit that precision. The z position precision is better than a half millimeter, depending on the tension in the thread. The best level of tension is low (under 2 lb), and vibrations are minimized when the thread touches but does not rotate the middle idler pulley on the stand shown on the right side of figure 1. Absolute z position is measured from the bead to

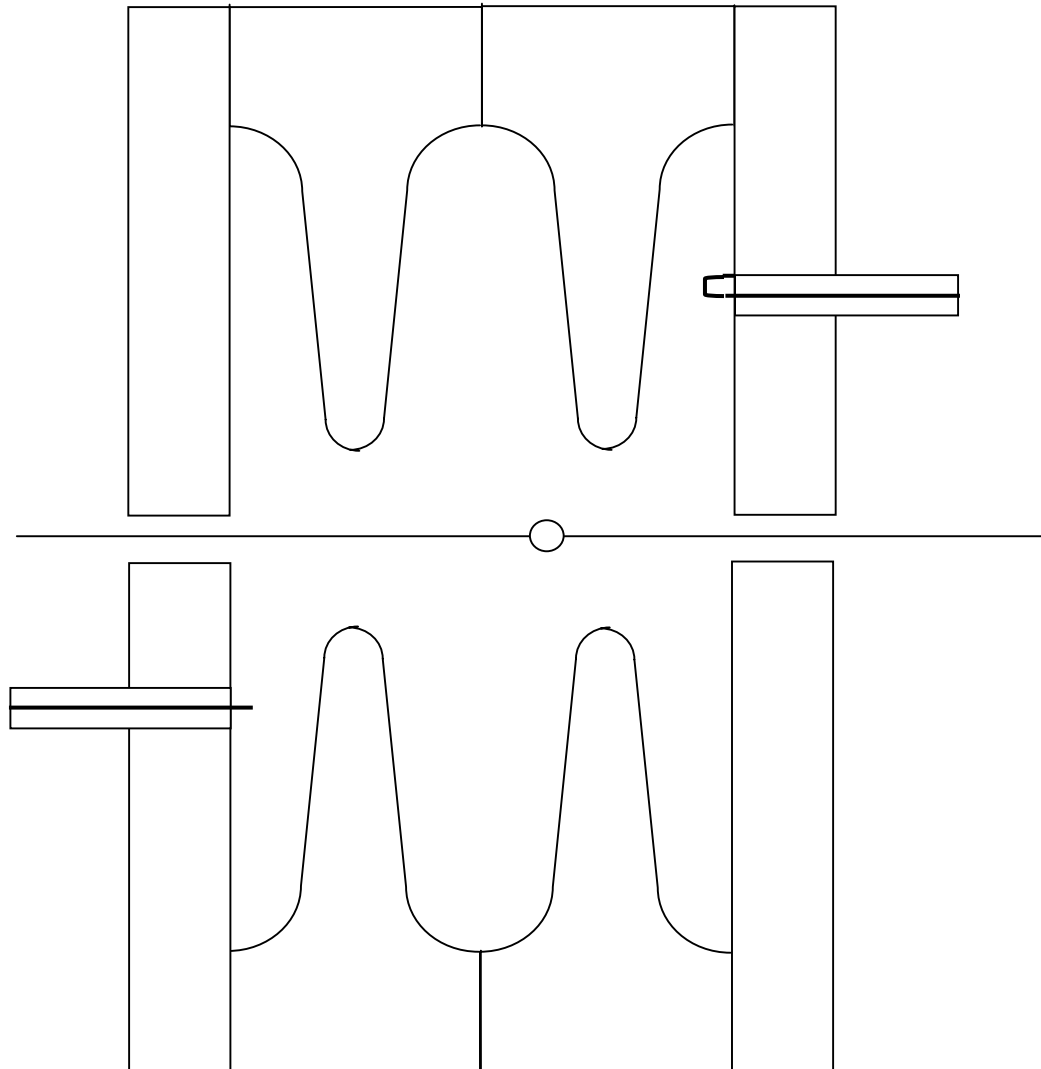


Figure 2. Cross sectional view of a two dumbbell stack with endplates and coupling and bead. At lower left, electric coupling produced with a stripped coax. The bare end is typically 1mm long. At upper right, magnetic coupling with a loop. The loop is typically 1mm radius.

the endplate when the bead pull is finished, with an uncertainty below a half of a millimeter.

The thread is a nylon monofilament line, 0.14mm in diameter before being put under tension. Its insertion into the 4-dumbbell cavity shifts the resonance of the π deflection mode down by 40 kHz. Some of this shift is no doubt due to measurement error – see section 4d.

The network analyzer was calibrated with the HP85033C test kit, using a full 2

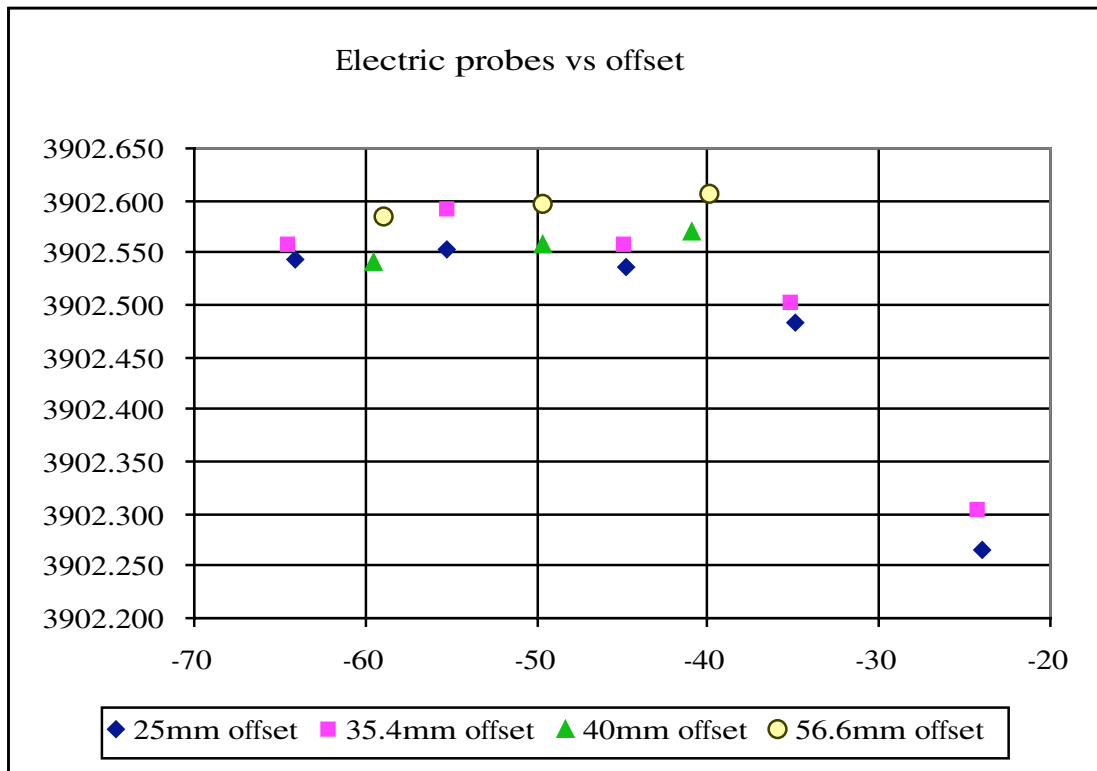


Figure 3. π deflection mode frequency (in MHz) of 4 dumbbell stack as a function of insertion loss (in dB) with electric coupling. The insertion loss is adjusted by moving the probes further in or out of the cavity; the 4 sets of points correspond to 4 sets of offsets of the probes position from the center of the cavity.

port calibration scheme. This had little effect on many of the measurements.

The π deflection mode frequency measurement was measured over the 3900.5 to 3903.5 GHz range with calibration both in place and not used; the results were consistent to 5kHz. In part this is due to a characteristic of the HP 8341B RF synthesized source: when the ramp is less than 5MHz in range, phase locking (and thereby better frequency measurement) is obtained at each point in the ramp. All measurements presented here were taken with calibrations in place unless otherwise noted, although some of the calibration sets used ramp mode and therefore could have some frequency scale problems.

2) Coupling and Q

Figure 2 shows a cross section of a 2 dumbbell stack and sketches two kinds of coupling devices. Both magnetic and electric probes have been used. Figures 3 through 6 show the measured frequency of the π deflection mode with various

coupling schemes. The probes are inserted until their outer conductors are flush with the inner face of the endplates and are then slowly withdrawn to

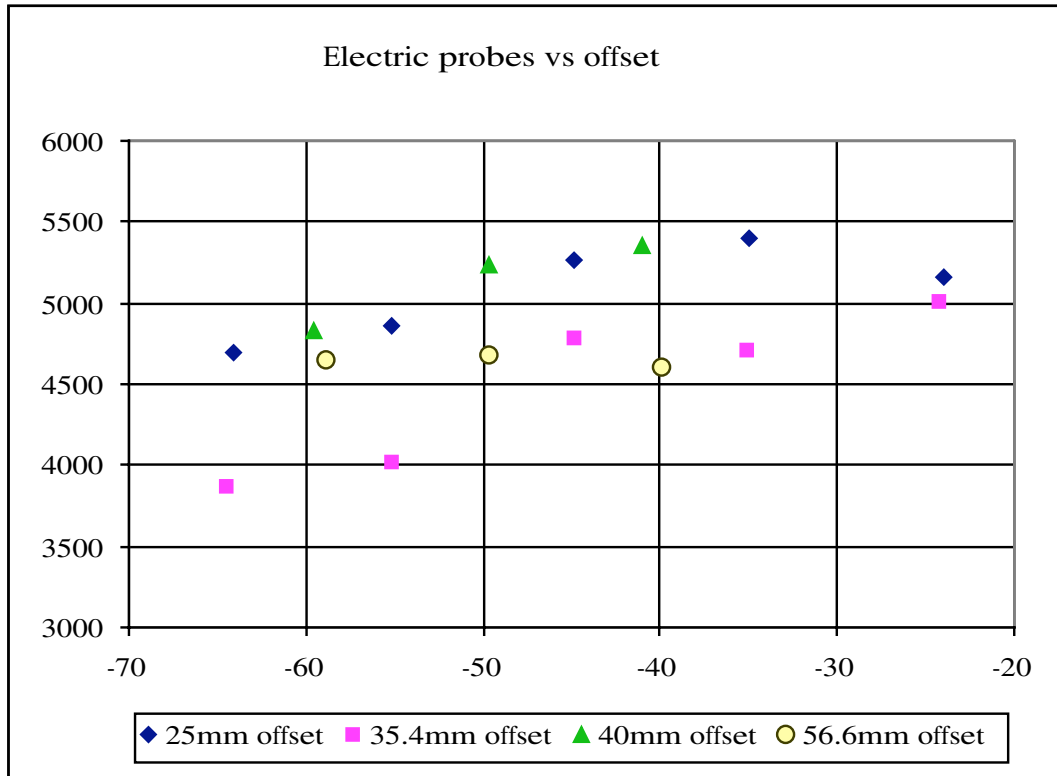


Figure 4. As in figure 3, but the y axis shows Q values.

reduce the coupling. For reasons which are not entirely clear, the use of electric coupling with the probes fully inserted 40mm off the axis of the cavities provides a good Q (5350 in this set of measurements) with a minimal shift in the resonant frequency – perhaps 30kHz worth. All of the measurements presented from here on out are made with this probe arrangement. The electric probe's inner conductor is about 1.8mm long and 0.92mm in diameter. The outer conductor has an inner diameter of about 2.5mm and an outer diameter of 3.55mm.

As may be seen from figures 4 and 6, Q values over 5000 are easily obtained. The key to obtaining these values was to use 1/2" thick endplates (which are not easily deformed) and to adjust the compression pressure of the stack while watching the shape of the peak on the network analyzer. Not a great deal of torque was needed to obtain the maximum resonance amplitude, which corresponds to the best Q. Nor was any additional polishing of the inner surfaces apart from what was done in their construction needed. Occasionally, the inner surfaces were wiped down with a paper tissue carrying WD-40 degreaser. However, Q values are hard to get precise and repeatable measurements for; a variation of ± 150 in measurements made in quick

succession has been observed. A Q of roughly twice the observed values is expected; presumably, there is still significant resistance across the interdumbell gap.

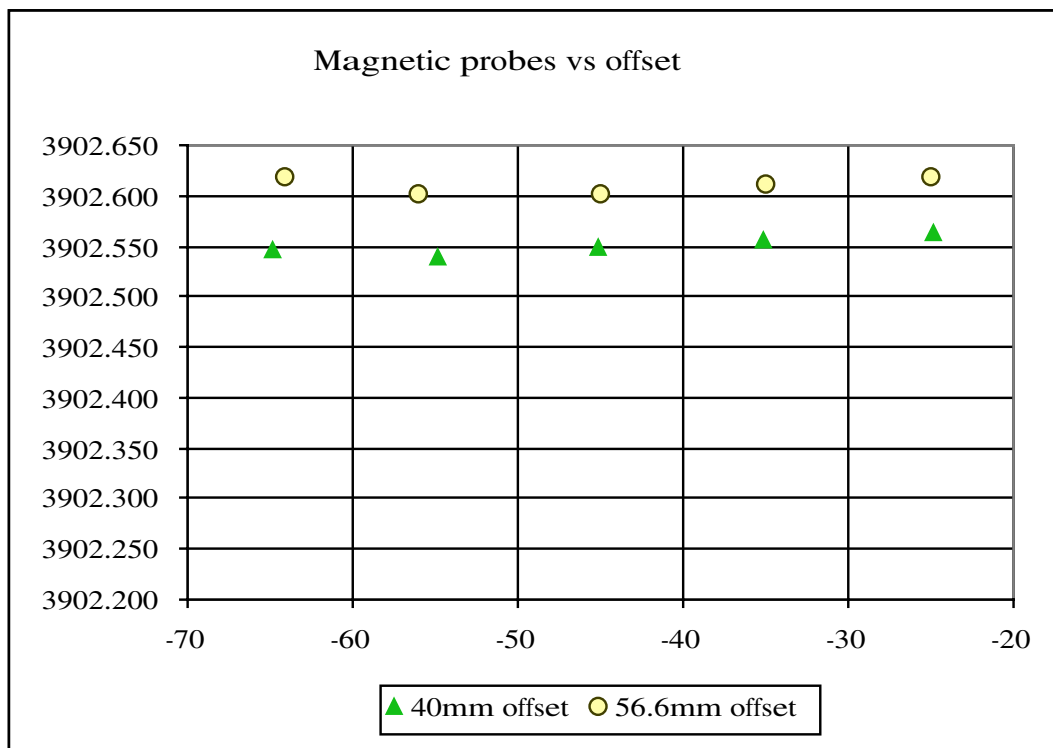


Figure 5. As in figure 3, but with magnetic coupling. Magnetic coupling at 35.4 and 25mm offsets distorted the resonant peak structure so much as to be unusable.

Q is relevant for at least two reasons. The first is that the physical size of the bead should be adjusted to match it; the bead should perturb the cavity so little that the shift in frequency from the bead is much less than $(f_0/2Q)$. The second reason lies in the relationship between the phase and the frequency for a simple resonant circuit.

$$f = f_0 + f_0/(2Q) \tan(\varphi - \varphi_0) ,$$

where f_0 is the resonant frequency and φ is phase of e.g. S_{21} in a transmission mode measurement, or Z in an RLC equivalent. The bead pull algorithm finds the peak frequency with the bead outside of the cavity, and defines the phase at that point as φ_0 . The bead is stepped to a sequence of positions and the phase is measured at each position. It is possible to average a number of

Magnetic probes vs offset

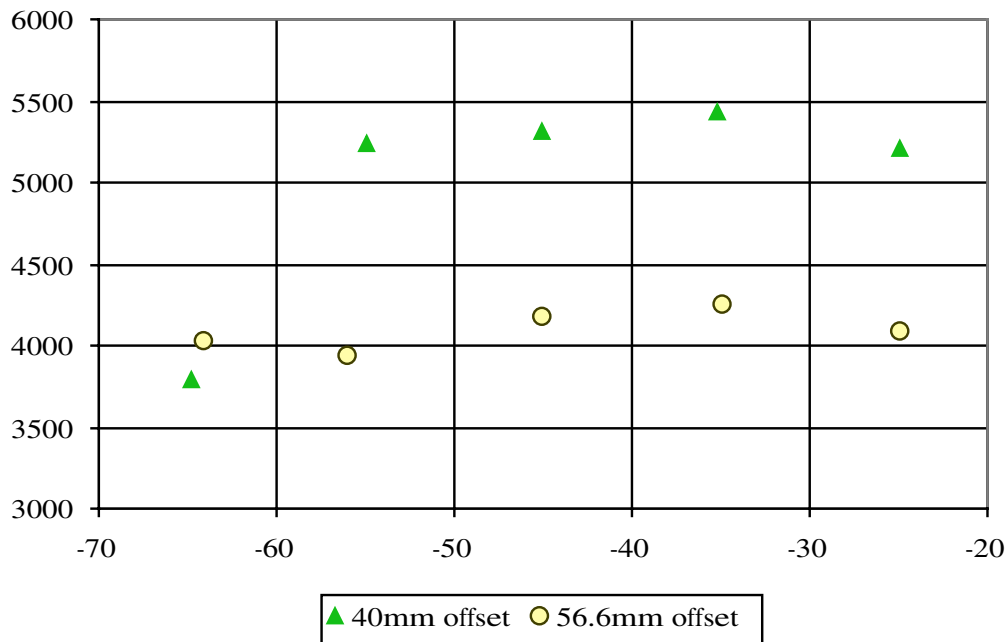


Figure 6. As in figure 4, but with magnetic coupling.

readings of the phase at each point, although this is not usually done. As a result, the phase shift measured near the resonant frequency is nearly proportional to any small shift in the resonant frequency, and the conversion is given by

$$(\pi f_0) / (360 Q) \text{ Hz / degree.}$$

Typical conversions are on the order of 7kHz per degree of phase shift, which is comparable to the 10 kHz IF bandwidth of the HP 8510 network analyzer. A final minor point is that in principle the sweep time of the network analyzer must be adjusted to the Q of the cavity; it must be much greater than Q / ω_0 , the decay time of the cavity. This condition is easily met for normally conducting cavities.

3) Ambient conditions

The frequencies of a cavity tested in ambient atmospheric conditions depends markedly on those conditions. Temperature changes will expand or contract the cavities and change the frequencies in proportion to the linear coefficient of expansion for the material used in constructing the cavities. Water in the

atmosphere will change the dielectric constant of the volume in the cavity. At this time, the temperature, barometric pressure, and relative humidity are measured with standalone devices and their values are used to correct the measured frequency to the frequency that would be measured in a vacuum at 25° C. The calculation is in an Excel spreadsheet, but here is the basic methodology.

From the temperature T in degrees centigrade, the vapor pressure V is found from an empirical fit to data taken from the CRC handbook:

$$V = 5.7232 \exp\{ (0.053546 T) + 1.6878 + 0.23539(T-24) + 0.00544721(T-24)^2 \}$$

The partial pressure of water P_W is found by multiplying V by the relative humidity; the partial pressure of dry air P_A is found by subtracting the water from the total air pressure. Then the dielectric constant is taken to be

$$\kappa = 1 + 210 \times 10^{-6} (P_A/T_K) + 180 \times 10^{-6} (1 + 5580/T_K) (P_W/T_K)$$

where T_K is the temperature in Kelvins. The measured frequency is multiplied by a factor of root κ and $(1 + \alpha(T-25^\circ\text{C}))$, where α is the linear coefficient of thermal expansion. There is also a known effect from CO_2 in the atmosphere. It has not been measured for in this work, but the correction formula, as given by Essen & Froome, Proc. Phys. Soc. B64 (1951) 862 is

$$\sqrt{\kappa} = 1 + 103.49 \times 10^{-6} (P_A/T) + 86.28 \times 10^{-6} (1 + 5748/T) (P_W/T) + 177.4 \times 10^{-6} (P_{\text{CO}_2}/T).$$

The precision of the atmospheric measurements is good, but the accuracy is still a slightly speculative matter. Temperature is measured with a Fluke model 80T-150U thermistor, which is accurate to $\pm 1^\circ\text{C}$; it is actually readout to a precision of $\pm 0.01^\circ\text{C}$. Barometric pressure is read with a mechanical device to better than a millibar, but the accuracy of this unit is not really known. Similar devices have an advertised accuracy of ± 1 mbar. Relative humidity is measured with a model HI8565 stick hygrometer manufactured by Hanna instruments. This model is no longer made, but Hanna's entire current line is spec'd to $\pm 2\%$ accuracy. The time needed to pull a bead through a cavity is on the order of a few minutes, and ambient conditions do not fluctuate greatly in that time frame. Bear in mind of course that there is no precisely known temperature at which the cavities were manufactured.

The inaccuracies and imprecision in a frequency measurement due to atmospheric measurement uncertainties can be estimated. Starting with a typical frequency measurement of the π deflection mode of 3901.710 MHz at 22.25° C, 995.0 mbar and 50% relative humidity, and varying the atmospheric parameters by 1° C, 3mbar, and 2% humidity in quadrature reveals that the corrected frequency is accurate to ± 95 kHz. The precision, *i.e.*, repeatability, is an order of magnitude better than that. These numbers are to be compared with the 40kHz shift from the presence of the thread, the 10 kHz IF bandwidth of the network

analyzer, the typically 7 kHz resolution of the frequency as measured with the phase shift, and the order of 30kHz shift due to probe loading. The Tesla project plans to allow an adjustment in the cryostat of 750 kHz for their superconducting cavities, and we will no doubt need to develop a similar device at some point in the future.

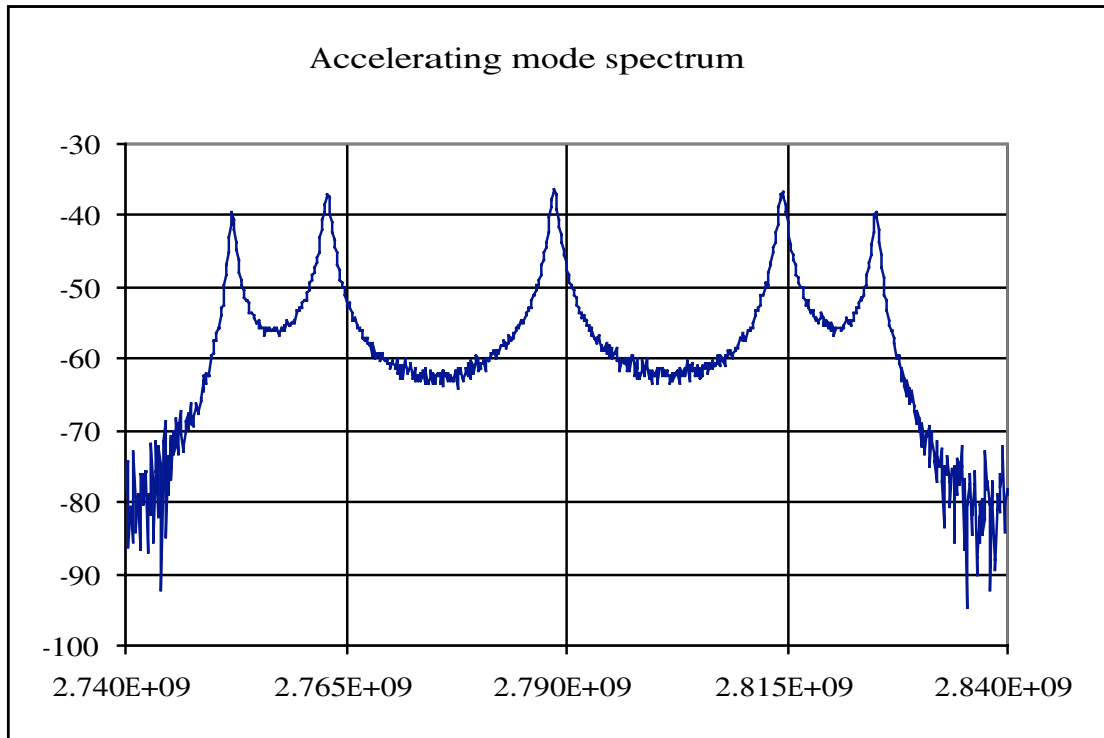


Figure 7. The accelerating mode (TM_{010}) spectrum for the 4 dumbbell stack. The vertical scale is insertion loss in dBm, and the horizontal scale is frequency in Hz.

4) The stack of 4 dumbbells

A stack of four dumbbells was tested extensively. These dumbbells are 'A15' prototype dumbbells; their equatorial diameter is 94.38mm, and the iris diameter is 30.00mm, with an iris curvature radius of 3.31mm.

a) Accelerating modes

Figure 7 shows the accelerating mode (TM_{010}) spectrum in the 4 dumbbell stack. This plot was taken without a calibration, but the network analyzer was in the step mode, where the RF source is phase locked at each frequency before measurement, so the frequency scale should be fairly reliable. The probes were

fully inserted with a 25mm offset from axis to improve the coupling to this mode. After correction for atmospheric conditions, the 5 peaks were found to be at 2752.703MHz, 2763.483MHz, 2789.217MHz, 2815.093MHz, and 2825.712MHz. Simulation with MAFIA gives a center frequency which is too low by about 0.15%, and a spacing between the modes which is too large by 1.07%.

The results of pulling the brass bead through the center of the stack for the 5 peaks are shown in figured 8 and 9. The brass bead is a bit too large to fully satisfy the small-perturbation criterion, but the features are clear. These features all appear in MAFIA simulation, including the non-zero offset in the $\pi/5$ mode and the inflection points in the $2\pi/5$ mode. However, scale of the frequency shift is not yet quite right in my simulation. Frequency shifts in MAFIA are systematically lower, typically a factor of 0.6 times the shifts in the data. The Q values for these 5 modes have not been measured carefully, but are on the order of 4400, so each degree corresponds to 7.75 kHz or so for small angles. Notice that the compensation for end cell effects is not perfect; each of the 5 modes shows a shift back towards zero phase – *i.e.*, to the unperturbed state when the bead is within a bead diameter of the endplates.

b) Higher modes - classification

Figure 10 shows the spectrum of deflecting (TM_{110}) and higher order modes in the 4 dumbbell stack. This plot was taken without a calibration, but the network analyzer was in the step mode. The peak on the far left is in fact a double peak, one of which is the deflection π mode. The structure near 5.42GHz contains 5 peaks spread symmetrically over a span of 50.6MHz.

At higher frequencies, the spectrum rises to a peak at 5913.293 MHz, and a complex spectrum exists at the highest frequencies. MAFIA shows the TM_{020} band begins at about 5899MHz.

Further information about these modes can be gathered by observing the relative strengths of the different peaks with different probe positions. Figure 11 shows the endplates. The large hole is the one used for passing the bead down the centerline of the stack; the red hole holds one of the electric probes, which creates a dipole perpendicular to the paper.

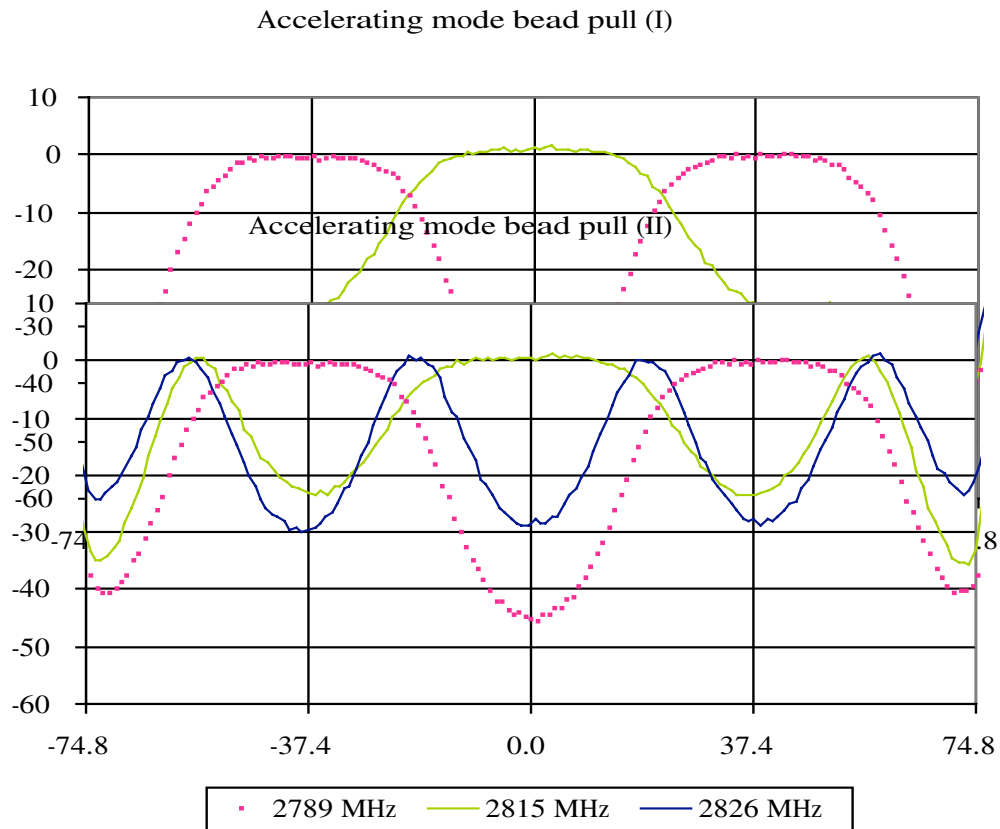


Figure 8. Bead pull results for the 3 lowest of the 5 accelerating modes of the 4 dumbbell stack. The brass ball bead and coupling as for Fig. 7 was used. The vertical axis is phase advance in degrees; the horizontal axis is bead position in mm from the center of the stack.

Figure 9. As in figure 8, but for the 3 highest of the 5 accelerating modes.

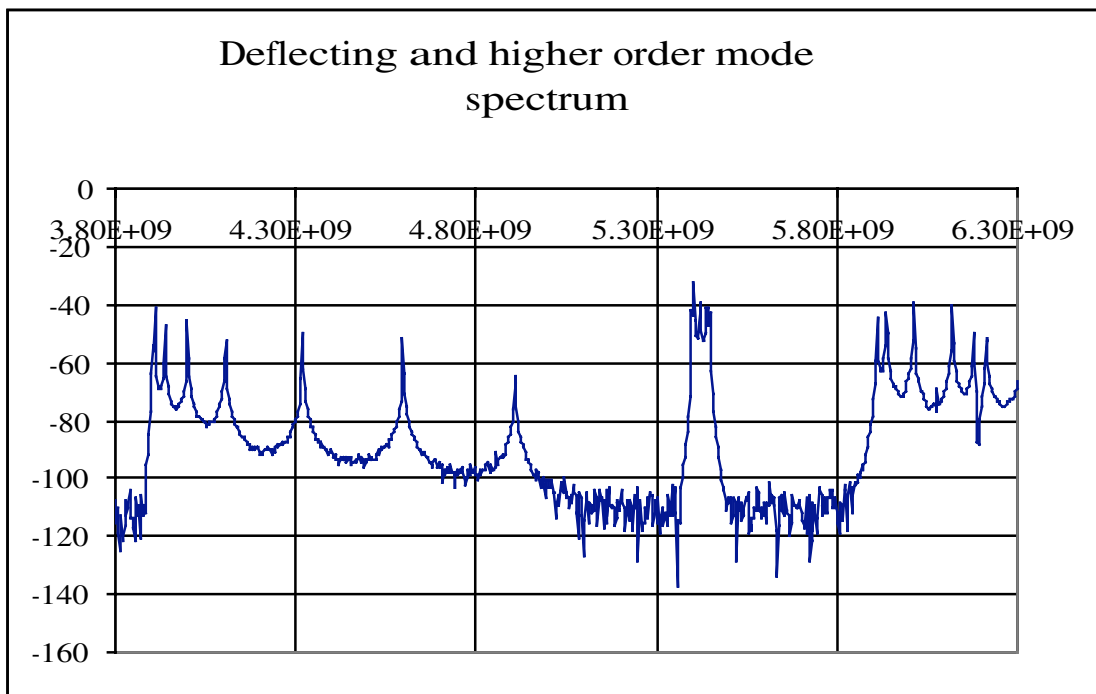


Figure 10. The deflecting and higher order mode spectrum of the 4 dumbbell stack. The vertical scale is insertion loss in dBm, and the horizontal scale is frequency in Hz.

Grey to Red hole,
4cm; Grey to
intermediate White
hole, 1inch. Grey
hole, 1/4". Other
holes 1/8"

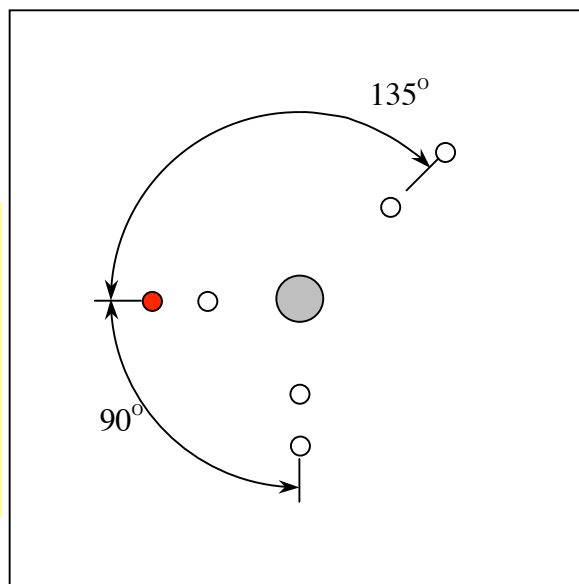


Figure 11. Sketch of endplate hole locations.

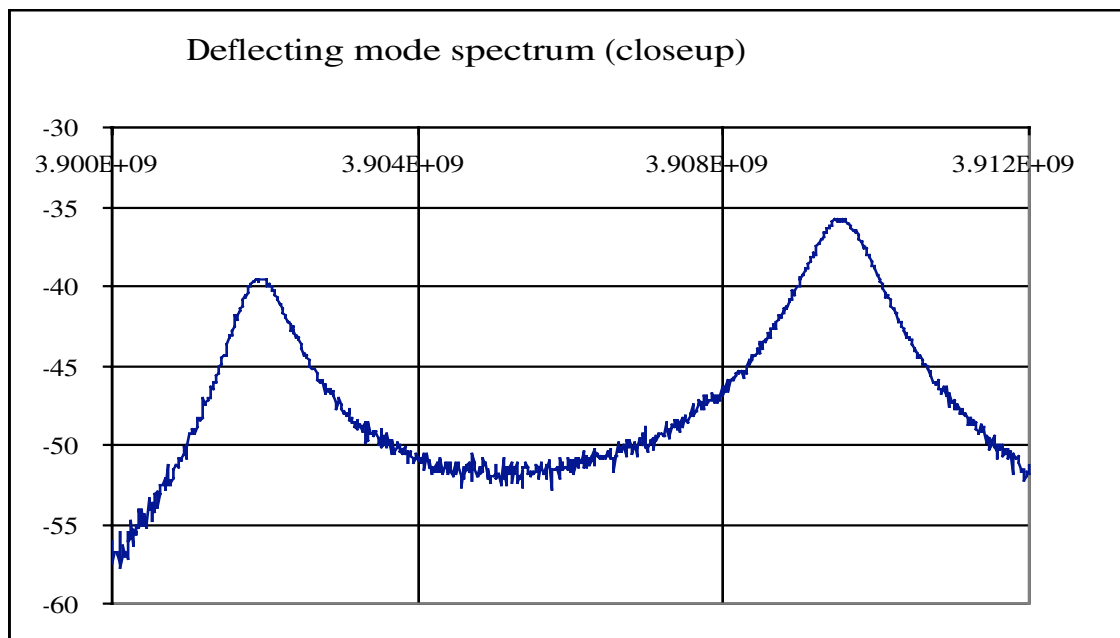


Figure 12. The first two peaks of the deflecting mode spectrum. The vertical scale is insertion loss in dBm, and the horizontal scale is frequency in Hz.

The two lowest frequency peaks are shown in detail in figure 12. Their corrected frequencies are 3902.810 MHz and 3910.404 MHz. There is little significant effect on Q as measured for the lowest frequency peak (the π mode peak) from the next peak; the -3 dB points are essentially symmetrically placed. The π deflection mode is found to be lower in MAFIA than in the data, by 0.14%, which corresponds well with the shift in the accelerating mode. The coupling is harder to simulate. In MAFIA, the spacing is too large, by 6.41%. Perhaps the coupling in the vicinity of the iris through the B field is hard to simulate well due to the tight geometry here. The next 3 peaks (measured without a calibration, but with the network analyzer in step mode) are at 3939.336MHz, 4001.342MHz and 4106.164MHz. All five of these resonances become quite weak when the other electric probe is placed on either of the holes at 90° to the other probe. These five resonances are the deflecting mode band.

The next three peaks are at 4320.246MHz, 4598.458MHz and 4909.105MHz. This is the region where the first higher-order mode (TE_{111}) is expected, but it is surprising to see only 3 peaks. From MAFIA we learn that the other two modes are up around 6196 and 6324MHz. In the pure TE modes, there can not be a longitudinal electric field on the equatorial plane of the cell, but that is how I had arranged the input and output couplers. Effectively, the system has only three cells. Like the deflection band, these modes are weak when the probes are placed 90° apart.

The five peaks near 5.42GHz are at 5398.686MHz, 5404.623MHz, 5421.752MHz, 5440.189MHz and 5449.295MHz. These resonances are enhanced when the probes are 90° apart, and weakened when the probes are 135° apart. Simulation with MAFIA reveals these to be the TM_{210} mode.

c) Higher order modes – bead pull results

Figure 13 shows the raw bead pull data taken at the π deflection mode resonance with the three different beads pulled down the center of the cavity. It is apparent that there are drifts, even over the 5 minute time span needed to take the 720 measurements in each of these plots. The drifts are comparable in magnitude to the drifts induced in variations in atmospheric conditions between the three runs, which were taken over a period of about two and a half hours. It is also apparent that there is either E_z (or $E_{x,y}$ or $B_{x,y}$) in the needle data which is largest at the iris region; MAFIA says that there are strong E_x fields in this region.

Figure 14 shows fully corrected bead pull results for the π deflection mode. The data taken with the bead well outside the cavities was fit to a line, and the resulting estimate of the drift subtracted out. The phase shift was re-expressed as a frequency shift using the value of Q (5266) measured at about the same time as the data were taken. The frequency of the initial measurement was corrected for atmospheric conditions and added back to all the subsequent measurements. Only the regions where the bead is inside the cavities is shown. There appears to be some shift in the z scale for the data with the brass bead. Notice also that the dielectric bead and the needle data have similar shapes, suggesting that the needle is actually measuring an electric field – a transverse one, from the MAFIA field maps.

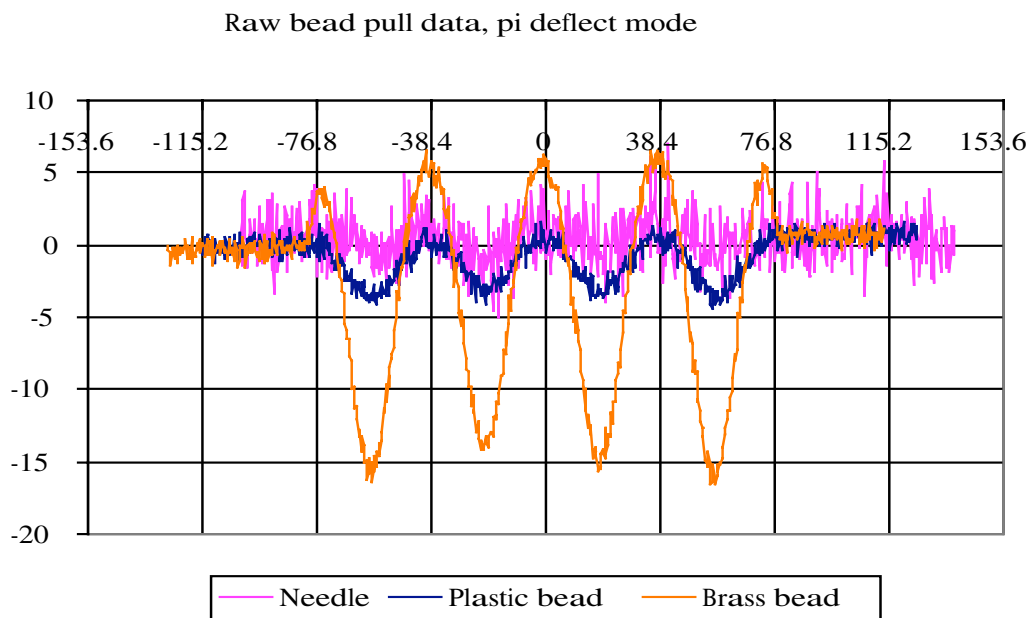


Figure 13. Raw data from bead pull in π deflection mode down center of cavities. The vertical axis is in degrees, and the horizontal axis is in mm.

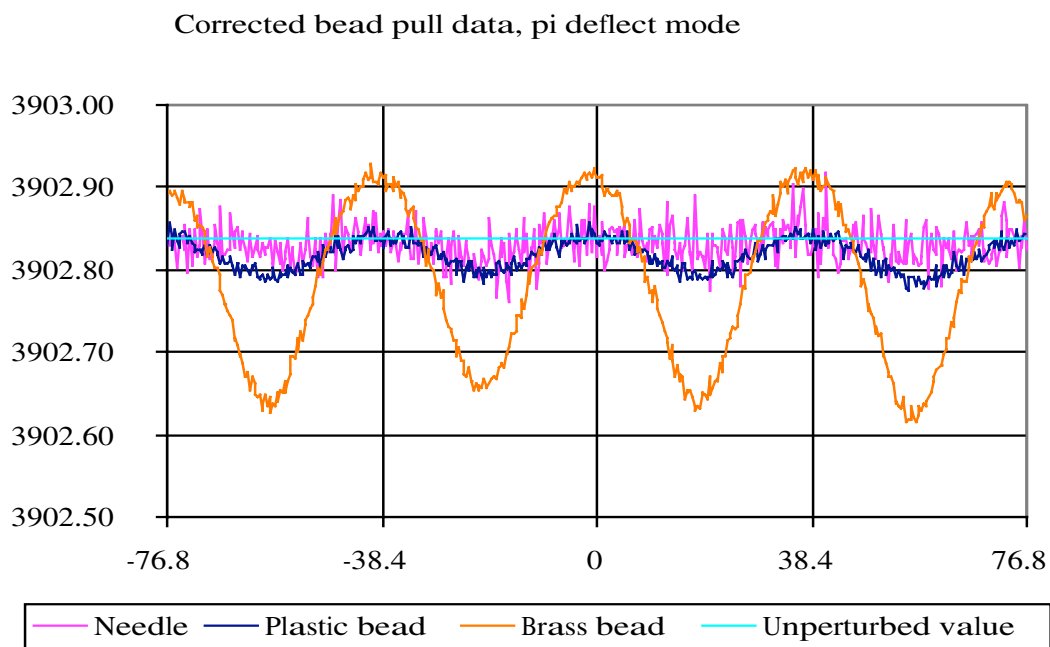


Figure 14. Fully corrected bead pull results for the π deflection mode. The vertical axis is in MHz, and the horizontal axis is in mm.

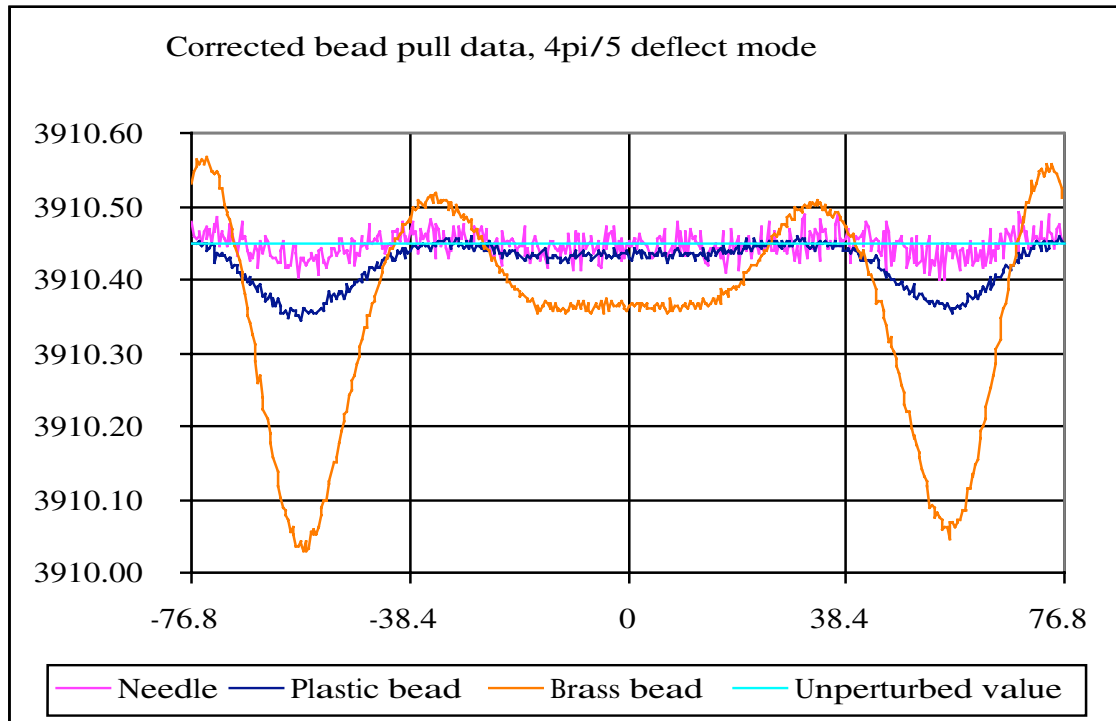


Figure 15. Fully corrected bead pull results in the $4\pi/5$ deflection mode down center of cavities. The vertical axis is in MHz, and the horizontal axis is in mm.

Figure 15 shows fully corrected bead pull results for the $4\pi/5$ deflection mode. The z scale problem seen in the π mode has disappeared. The largest phase shift excursion is 25° , which is larger than the perturbative requirement, but not by much.

MAFIA plots show excellent qualitative agreement with the results of Figures 14 and 15, as well as with the results shown in Figure 18. However, as in the accelerating mode, the frequency shifts are too small in the simulation. The MAFIA Δf values are a factor of roughly 5 smaller for the metallic beads, and a factor of 9 smaller for the dielectric bead. Actually, the dielectric constant for the plastic bead is not known and was not factored into the simulation; the result corresponds to a bead with very high dielectric constant.

Figure 16 shows partially corrected bead pull results for the second TE_{111} mode, which is at 4598 MHz. The phase shift reaches 90° , much greater than the perturbative requirement allows. As a result, these data are useful only to qualitatively describe the modes. The plots have been corrected for long term drift.

Figure 17 shows the fully corrected bead pull results for the central mode in the structure tentatively identified as the TM_{210} band. There appears to be no

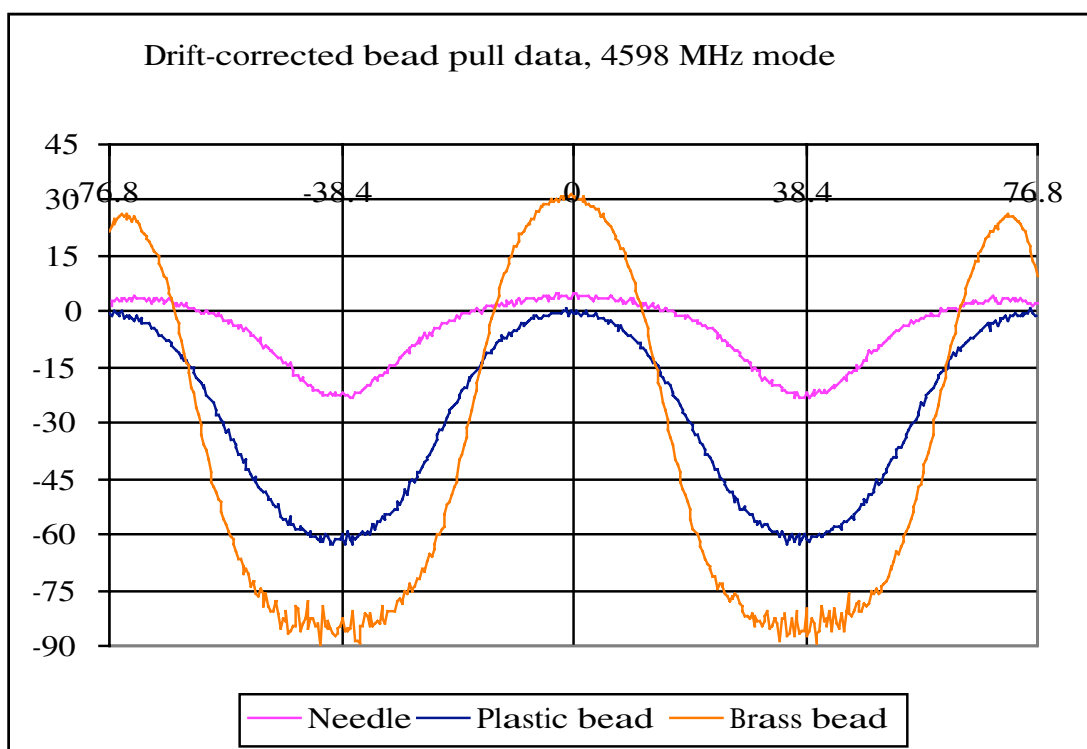


Figure 16. Drift-corrected bead pull results for the second TE_{111} mode. Vertical axis is in degrees, horizontal axis is in mm

field to speak of along the axis in this mode, a result confirmed by MAFIA.

d) π deflection mode – off-axis bead pull results

After the other measurements described here were done, a new set of holes was drilled in the endplates which allowed running a bead down a line parallel to but 12mm from the axis of the four dumbbell stack. The new axis was 180° degrees from the probes shown in figure 11.

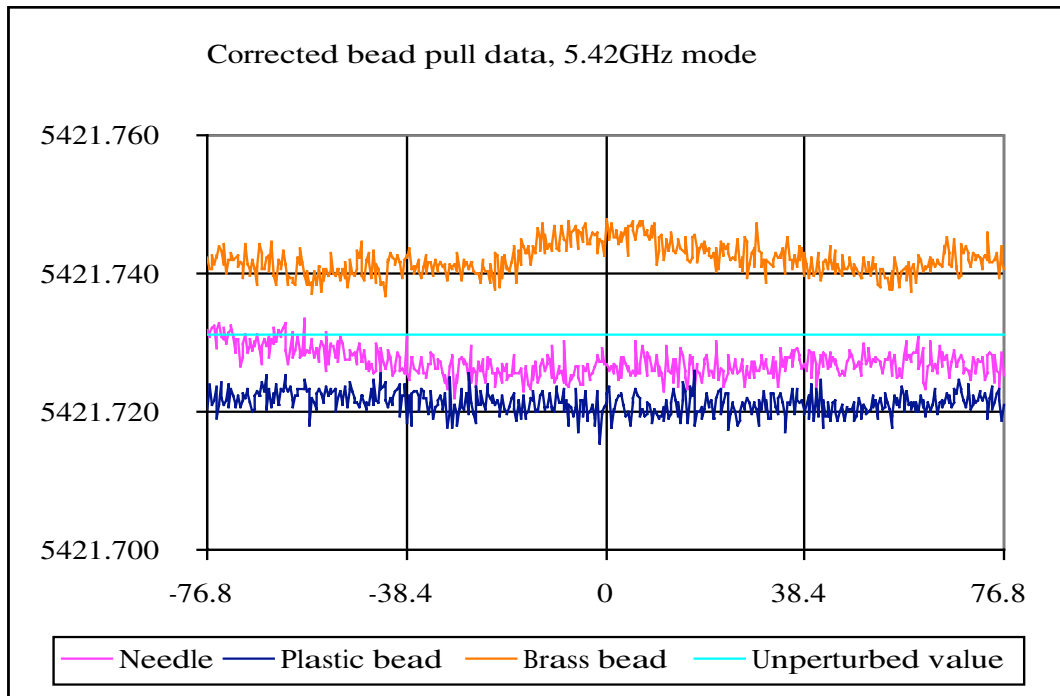


Figure 17. Fully corrected bead pull results for the central mode in the structure at 5.43 GHz. Vertical axis is in MHz, horizontal axis is in mm.

The resonant frequency, corrected for atmospheric conditions was measured to be 230 kHz higher than the value when the thread was in the center of the stack. This result is physically impossible. In principle, there could be a shift due to the dielectric of the thread being immersed in a region of higher field – recall that a 40 kHz shift was seen simply by inserting the thread down the axis. From Figure 14, a 40 kHz shift occurred when the plastic bead was at the iris. The volume of the thread inside the stack was 2.36 cubic millimeters, *i.e.*, about 40% of that of the bead. The curve for the bead is roughly sinusoidal, so the perturbation for the thread should be about $(1/2)(40\%)(40 \text{ kHz}) = 8 \text{ kHz}$. The maximum electric field in the iris is 0.284 V/m in the MAFIA simulation (no peak field normalization has been done) and around 1/2 V/m in the region where the offset thread was placed. That means that there might be a shift due to the insertion of the thread off-axis on the order of 30 kHz.

Figure 18 shows the fully corrected results. For the needle and the red dielectric bead, the largest perturbation corresponded to a phase shift of 20 to 25°, only slightly larger than desired. For the brass bead, the maximum phase shift was more like 55°. It is gratifying to see that the needle plots a field which is reasonably uniform inside each cell. Note that the electric field never goes to zero along this thread, so the plastic bead's trace can not be used to

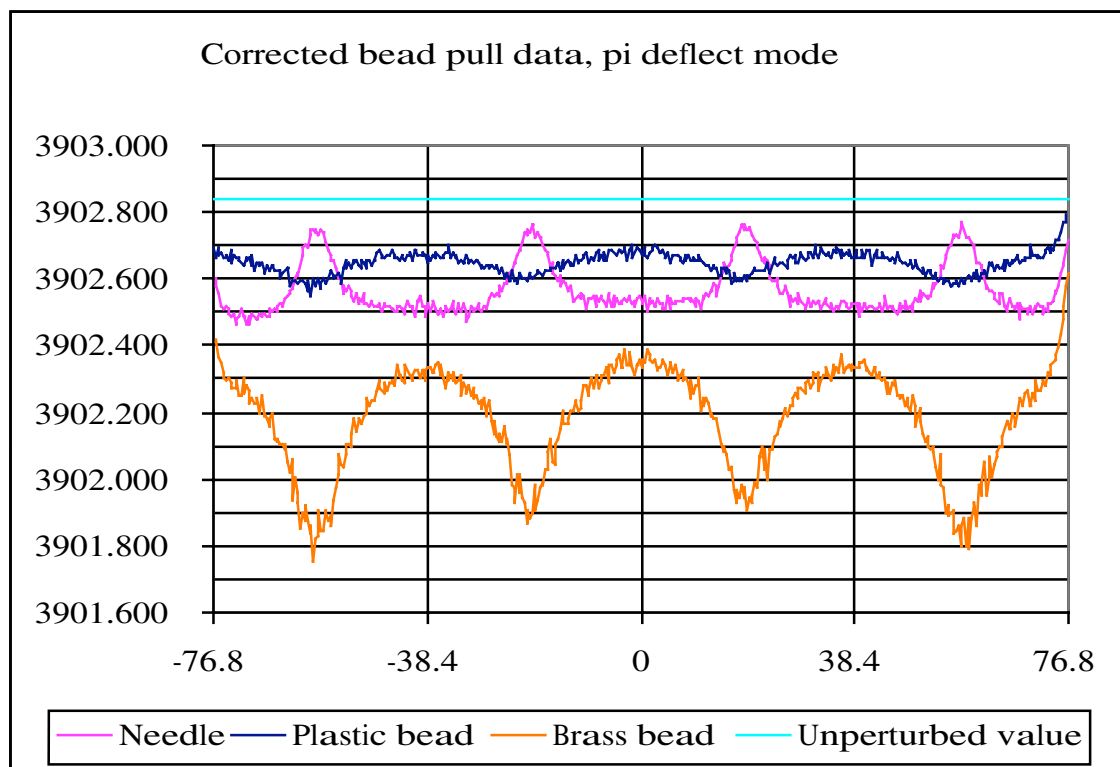


Figure 18. Fully corrected bead pull results for the π deflection mode, with the bead 12mm off the central axis of the stack. The vertical axis is in MHz, and the horizontal axis is in mm.

confirm the unperturbed frequency. The unperturbed value shown is 3902.810 MHz, from the measurement before the thread was inserted.

5) The elliptical dumbbell

We also have an elliptically polarized dumbbell, where the diameter in the horizontal direction is 95.85mm and the vertical diameter is 95.30mm (the nominal A15 design is 94.38mm). This cavity did not for some reason exhibit Q values as high as the four dumbbell stack; Q over 3000 has yet to be obtained. Figure 19 shows the spectrum of higher order modes, when this system is excited with electric probes placed at the holes marked in red on figure 11. The network analyzer was not calibrated for this plot, but the RF source was in step mode. Conspicuously, the TE_{111} modes are absent, as would be expected, given the driving structure. The structure which appeared at 5.42 GHz is prominent and appears at about 5.36 GHz here. The deflection mode band is the two peaks at the left of figure 19. It is shown in greater detail in figure 20.

The four peaks in figure 20 are at (after correction for atmospheric conditions) 3848.80 MHz (π mode, horizontal deflection), 3869.55 MHz (π mode, vertical deflection), 4045.08 MHz (0 mode, horizontal deflection) and 4070.02 MHz (0 mode, vertical deflection). The frequency splitting is thus 0.538%; the geometric splitting is 0.575%. The uncertainty in the geometric splitting is on the order of 0.040%, so the numbers are equal. Figure 20 also shows the relative phase between the two cells as a function of frequency; the arbitrary offset is selected to make the phase zero in the region between the two resonances. For this data, the electric probes were placed 56.6mm off axis, on the diagonal at 135° shown in figure 11. This excited both polarizations approximately equally.

Since we have on hand only a single polarized cell, and it does not easily fit into the stack of four non-polarized dumbbells, available bead pull data for polarized models is not very interesting. However, as describe in section 4b above, we seem to be able to select the polarization reasonably well with probe positioning

Deflecting / H.O. mode spectrum, elliptical dumbbell

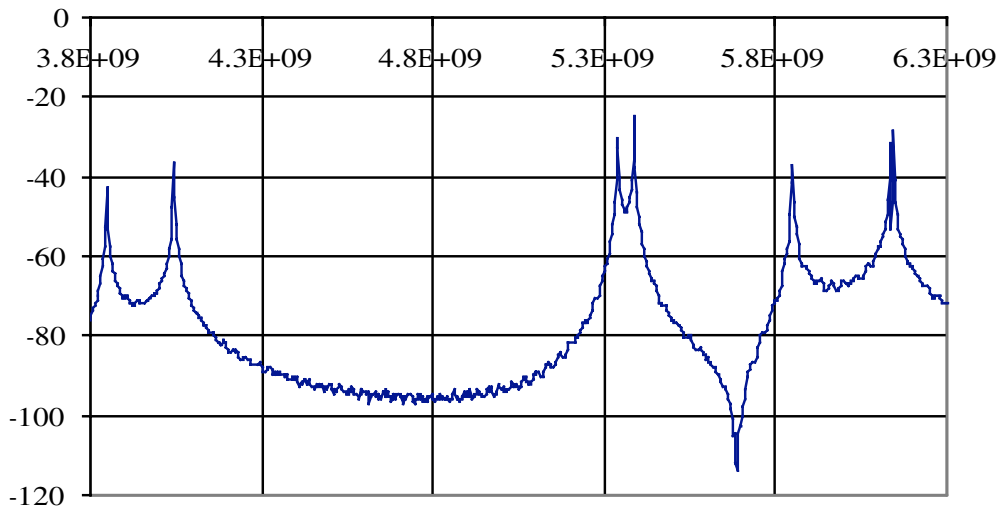


Figure 19. As in figure 10, but with a single elliptically polarized dumbbell.

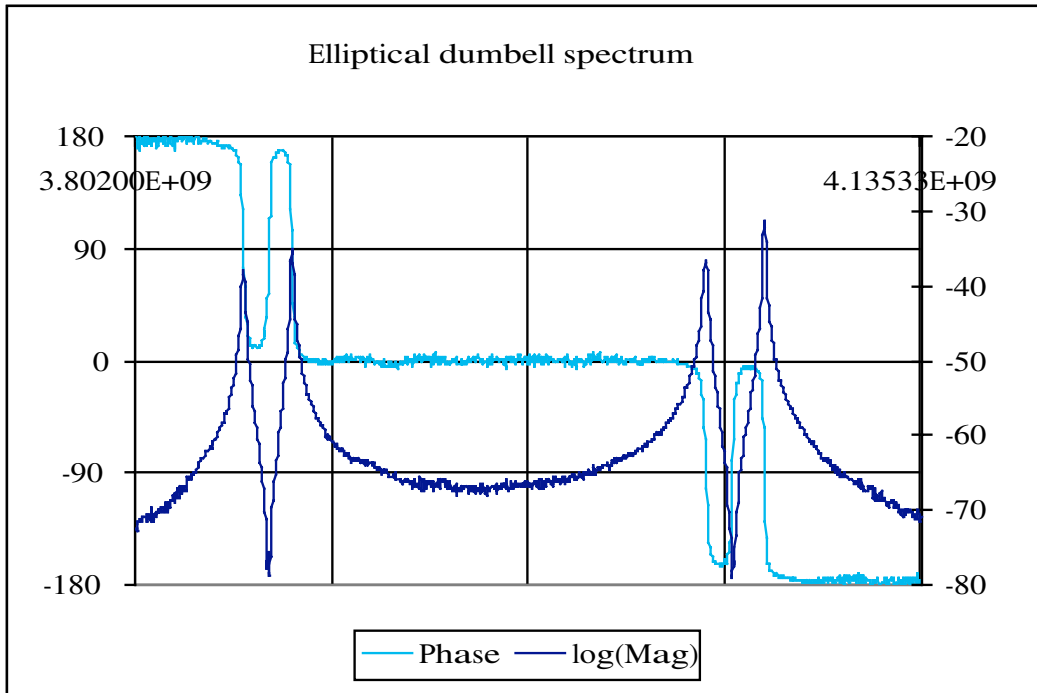


Figure 20. The deflection mode band for the elliptically polarized dumbbell. Vertical axis is degrees (for phase) and Hertz (for log amplitude); horizontal scale is in Hertz.

6) Location and description of the code to do all this

The code used to make the measurements presented here lives on the A0 bead-pull Mac, in the subdirectory of the MacOS partition named LeoView. In the subdirectory General Tests are the following LabView VIs:

- 1) Savesheet.vi: This VI starts the 8510's DAQ sequence – *i.e.*, a single sweep in frequencies – and prompt the operator for information regarding atmospheric conditions, his name, an output file name, and a comment regarding the data. A field containing frequency information exists but should be ignored. When the operator clicks the “continue” button, the data showing on the 8510 is transferred to a spreadsheet file along with the header information. *This happens even if the 8510 has not finished the scan in frequencies.* If the readout of the data and construction of the spreadsheet happens before the scan has finished the subVI to close VISA I/O connection to the network analyzer will hang. Better to wait until the 8510 has finished taking data before hitting “continue”.
- 2) Measure Q.vi: This VI needs a valid calibration set to function, because of the sensitive nature of Q measurements. The selection of a calibration set in

the 8510 defines also a frequency range and DAQ mode. Within the range specified by the input calibration set, this VI looks for a peak using the Fine Measure subVI with default settings. It processes the data from that subVI to find the frequency, amplitude and ± 3 dB points of the single peak. From this it calculates Q, and sets a red warning light if the \pm dB points are outside the selected range.

- 3) Repeated peakfind.vi: This VI begins by interacting with the operator to select a particular peak. The procedure is to ask the operator “Can you measure that?” – the operator should say YES if there is a single clear peak near the center of the 8510 network analyzer’s screen. If the operator responds NOT, the subVI relinquishes control of the network analyzer and asks the operator to select his desired frequency range. The operator must then adjust markers 1 and 2 on the 8510 to span the entire range. After he does so, and tells the VI that he has done so, the VI will reassert control of the network analyzer and set the frequency range to run from marker 1 to marker 2. This having been done, Repeated peakfind.vi then looks for a single peak with the Find mode peaks.vi and then calls Fine measure.vi 32 times. The input central frequency for Fine measure.vi is the result of Find mode peaks.vi; the width is selected by a front panel control. Code exists to use a calibration set to select the frequency range, but there seems to be a bug in the firmware of the HP 8510 which makes subsequent calls unreliable. The manifestation of this bug is that the first result is correct and is markedly different from later results. Ultimately, the results of the Fine measure peak finding algorithm are presented, along with their mean and standard deviation.
- 4) Phase pull.vi: This is the central bead pull code. It begins with the same interactive dialog used in Repeated peakfind.vi to select the resonance to be measured. Then it does an initialization of the bead position with the Init bead.vi, followed by a measurement of the peak frequency. The resonance is found with a call to Find mode peaks.vi to find a single peak, and that is followed by a call to Fine measure.vi using the result of Find mode peaks for the central frequency and a frequency span of 2.5MHz. Once the resonance has been defined, Phase pull.vi prompts the operator for the information described above for Savesheet.vi, and puts the network analyzer in the single-frequency DAQ mode. The central loop of Phase pull.vi positions the bead in increments specified on the front panel and then takes a measurement of the phase of S_{21} . The first measurement of that phase is taken to be the phase offset, so all later measurements are relative to the first point. An ABORT SCAN button will terminate this loop, but no output will result if it is used. As in Savesheet.vi, the data is stored in a spreadsheet with the commentary information on the top.

The Labview VIs in the General Tests area use subVIs in the MacOS : LeoView : Util VIs area. The most important ones are:

- 1) Find mode peaks.vi: This VI locates an arbitrary (but usually 1 or 5) peaks or dips (in principle – that feature has never been tested) with what is intended to be a robust if not precise algorithm. Four sweep averages are taken over whichever frequency range the 8510 has previously been set to scan. The Labview primitive peak finder is used to look for peaks in sets of 5 adjacent data points. Various cases for more than, less than, or exactly the requested number of peaks are handled. The sweep averaging is reset just before the subVI returns.
- 2) Fine measure.vi: This code is designed to produce a precise measurement of the frequency of a peak or dip (again, the dip features have not been used). An initial estimate of the frequency range must be provided. This can actually be specified as a calibration set by feeding the calibration set number into the subVI in place of an initial central frequency. This VI will install the calibration set if an integer value is found in place of the double precision frequency. Warning: some timing requirements in this code are critical to its correct functioning, and have not been tested for calibration sets or initial network analyzer states which have the analyzer working in step rather than ramp mode. The user may also specify the number of sweeps to average; the default is 16. The 8510 then takes an 801 point scan in linear magnitude mode, and looks for a single peak. The sweep averaging and number of points in a scan are reset just before returning.
- 3) Phase measure.vi: This VI is the heart of the bead pull algorithm. At a given frequency it reads the phase data. There is an input flag for the first call, which both sets the 8510 into single-frequency mode and takes the measured value and loads it into the phase offset register. The subVI MacOS : LeoView : Util VIs : HP8510 working : HP 8510 Collect/display datum.vi is used to get a pair of numbers; it is a modified version of the 8510 Collect/display data.vi in the same area.
- 4) The subdirectory MacOS : LeoView : Util VIs : HP8510 working contains modified copies of the HP8510B LabView drivers provided over the Internet by National Instruments as shareware. A number of modifications were made; some were necessary, some were merely cosmetic. Only those drivers needed to support the functions needed for this work have been put in this area.

The original versions of the HP8510 shareware are in MacOS : BEAD Pull System : Network Analyzer : hp8510b : HP8510B VI's, along with a great number of other VIs and supporting information. The BEAD Pull area also includes the LabView application and its supporting files and software for the serial port adaptor.

The atmospheric corrections are implemented as an Excel spreadsheet in MacOS : BEAD Pull System : Freq correct.

The code developed by Bob Flora for control of the stepper motor is in MacOS : BEAD Pull System : Position / Motor Control – the VIs themselves are in the subdirectory Motion VIs. Proof of Motion.vi and Serial Port Init.vi (it is in GALIL DMC-1412 Commands : GENERAL CONFIGURATION) are particularly useful for simple exercises in bead motion such as alignment to cavity position and discovering what you forgot to plug in or turn on.

Analysis of the data once taken is still relatively rudimentary. All the plots shown here were created by manually manipulating the spreadsheets created by the LabView code. In MacOS : LeoView : Data analysis is a spreadsheet which implements the five cell tuning algorithm of *Padamsee, Knobloch and Hays*, Chapter 7. That algorithm's input is measured frequency changes at the center of each cell, and its output is applied frequency changes for the next iteration of the tuning process.

Most of the MAFIA code used to study this data exists on FSUB01 in the FNALU cluster, in the area /afs/fnal.gov/files/home/room1/bellanto/MAFIA/alm-rz. Some is also in Mike McAshan's area; Rainer Wanzenberg's area of course contains an extensive collection of useful files.

7) Conclusions

I got me some data and it looks fairly reasonable. The frequency shifts due to inserting a thread seem incorrect, and my MAFIA calculations for the effects of a bead have some overall scale problems, but the qualitative and in many cases quantitative behavior is understood.

A second set of conclusions has to do with those various shortcomings in the present apparatus which we might choose to remove through various upgrades. Thread vibrations and the mechanical alignment of the cavities on the bead pull structure are clearly issues. Drift in the atmospherics – or something else - on the time scale of a few minutes is also evident in our data. We could use a few beads and needles of known dielectric and somewhat less than 3mm in size, but this is not crucial.

Again, analysis of the data once taken is still relatively rudimentary; making the plots for this note took far more time than collecting the data for it.

What have we learned in regards to tuning the 5 cell niobium structure? From the data presented here, the MAFIA plots referred to here, and various other considerations that have occurred to me as I wrote this:

- a) It is probably better to polarize before tuning. At the very least, polarization will distort the metal and perhaps make re-tuning necessary. Also, I would like to actually watch the process whereby multiple peaks in the deflecting modes are separated by carefully looking at the spectra before and after the polarization process before tuning.
- b) Tuning algorithms need a frequency shift due to the presence of the bead. If the thread has a significant effect, this has to be allowed for in the calculation (although the uniformity in the bead pull plot for the tuned cavity will still be obvious). That suggests that we pull a bead down the center, rather than down the side, or near the iris.
- c) The variation of the trace from pulling a needle down the center shows that a needle of practical dimensions responds to transverse electric fields. This also suggests that the interpretation of a needle pulled off-axis might be a little complicated, even though that gives a reasonably direct measurement of E_z , which is from a mathematical viewpoint an important quantity.
- d) In the center of the cell, for the deflecting mode, there is no electric field at all, and only a deflecting magnetic field. This is the field that determines the cavity's performance, and it can be directly measured with a metal bead. Ideally, a flat bead, oriented perpendicular to the field would directly measure only the deflecting field, but it will be quite tricky to keep such a bead from spinning around the thread's axis. A round metal bead is best. From Figure 13, the 3mm brass bead is of about the right size, more or less. The appropriate quantity to use in the tuning calculation is thus the distance from the peak of the orange curve in Figure 14 to the blue line, essentially.
- e) How well tuned does the cavity have to be? I do not really know yet.

The tuning of a deflecting mode cavity may be quite similar to the tuning of an accelerating mode cavity after all!

8) List of useful references

Padamsee, Knobloch and Hays, "RF Superconductivity for Accelerators", John Wiley & Sons, New York.

Maier and Slater, Journal of Applied Physics, Vol 23 (1952) p 68-77.

Edwards et.al., Fermilab TH-2060, November 1988.